Climate Dynamics (2019) 52:3845–3855
https://doi.org/10.1007/s00382-018-4363-4

Impact of the cross-tropopause wind shear on tropical cyclone genesis over the Western North Pacific in May

Jingliang Huangfu[1] · Wen Chen[1,2] · Maoqiu Jian[3] · Ronghui Huang[1,2]

Received: 15 November 2017 / Accepted: 11 July 2018 / Published online: 24 July 2018

Abstract
The role of the 50- to 200-hPa zonal wind shear in modulating tropical cyclone (TC) genesis over the western North Pacific (WNP) in May is investigated in this study. Concurrent with the strong cross-tropopause shear over the key region (0°–5°N, 160°–180°E), suppressed convection was observed over the tropical WNP, especially over the South China Sea and the Philippines. The monsoon trough (MT) was confined westward. However, enhanced convection occurred in the weak shear years and the MT extended eastward. This cross-tropopause wind shear is negatively correlated with TC genesis in May, with a decreased (increased) number of TCs corresponding to strong (weak) cross-tropopause wind shear.
This cross-tropopause wind shear can be treated as the combined impacts of the El Niño-Southern Oscillation (ENSO) events and the stratospheric quasi-biennial oscillation (QBO). When decaying El Niño events coupled with the easterly phase of the QBO were noted, the cross-tropopause wind shear was stronger with weakened convection, and an enhanced western Pacific subtropical high was observed. TCs are rarely generated during these years. In contrast, the modulation of the QBO westerly phase on decaying La Niña events is limited. Affected by the QBO westerly phase, TC genesis in the May following La Niña events is only slightly enhanced. The energy analysis indicates that the combined impacts of the decaying El Niño events and the QBO easterly phase might suppress the barotropic eddy kinetic energy conversion in May, whereas the decaying La Niña events and the QBO west phase act in an opposite manner.

Keywords Cross-tropopause wind shear · Quasi-biennial oscillation · ENSO event · Tropical cyclone genesis · Western North Pacific

1 Introduction

The tropical cyclone (TC) season over the western North Pacific (WNP) starts in May and ends after December (He et al. 2015). TC genesis over the WNP in May exhibits distinct characteristics from the peak period of typhoon season (Chen et al. 2017; Huangfu et al. 2017a, b). Huangfu et al. (2017a) noted that the numbers of TCs generated over the WNP in May increased after the late 1990s, which is consistent with the interdecadal early onset of the South China Sea summer monsoon (SCSSM) (Huangfu et al. 2015). This finding is in sharp contrast to the consensus that TC genesis is decreasing in recent decades during the peak typhoon seasons (e.g., Liu and Chan 2013). Huangfu et al. (2017b) indicated that the early onset of the SCSSM results in the eastward intrusion of the monsoon trough (MT) into the WNP, leading to increased TC genesis in May. Huangfu et al. (2017c) studied the effects of sea surface temperature (SST) in different tropical regions on TC genesis over the WNP in May. They showed that warmer SSTs over the tropical Pacific (Indian) Ocean in March lead to increased (decreased) numbers of TCs in May. Chen et al. (2017) investigated the impact of the summer monsoon westerlies on TC genesis in the South China Sea (SCS) in May and documented its genesis mechanism based on the eastward extension of the MT.

The El Niño-Southern Oscillation (ENSO) is an important precursor signal of the following TC season (Xie et al.

✉ Jingliang Huangfu
hfjl@mail.iap.ac.cn

1 Center for Monsoon System Research, Institute of Atmospheric Physics, Chinese Academy of Sciences, P.O. Box 2718, Beijing 100190, China

2 College of Earth Sciences, University of Chinese Academy of Sciences, Beijing 100049, China

3 School of Atmospheric Sciences, Sun Yat-sen University, Guangzhou, China

2009; Du et al. 2011). Xie et al. (2009) demonstrated that the El Niño-induced warming over the tropical Indian Ocean can lead to an anomalous Walker circulation reversal, inducing a persistent anomalous anti-cyclone over the WNP. Feng et al. (2011) suggested that this anomalous anti-cyclone can persist until the El Niño decaying summers. Du et al. (2011) reported that fewer TCs were generated during strong El Niño decaying summers. The aforementioned El Niño-related anomalous anti-cyclone might lead to a decreased number of TCs by restricting the eastward extension of the MT.

Several previous studies have also demonstrated that TC activity over different tropical oceans is modulated by the stratospheric quasi-biennial oscillation (QBO) (Gray 1984; Shapiro 1989; Chan 1995; Jury et al. 1999; Camargo and Sobel 2010; Goebbert and Leslie 2010; Fadnavis et al. 2014; Caron et al. 2015). Chan (1995) used zonal winds at 50, 30 and 10 hPa over Balboa (9°N, 80°W) to represent the QBO, suggesting that the westerly phase of the QBO (hereafter referred to as QBO_W; the QBO_E refers to the easterly phase of the QBO) corresponds to an increased number of TCs over the WNP during 1958–1988. As Gray et al. (1992) described, during the QBO_W (defined by the 30 hPa stratospheric winds), the deep equatorial convection is suppressed, whereas the off-equatorial monsoon convection is enhanced, supporting the increased TC genesis over the tropics. However, Ho et al. (2009) argued that the QBO and the number of TC genesis over the WNP tends to be insignificantly correlated during 1976–2007 with the QBO phases identified by calculating the vertical shears between the zonal winds at 50 and 70 hPa. According to Baldwin et al. (2001), the main periods of the QBO are approximately 27 months, which may explain the interdecadal instability of the relationship between the QBO signal and the interannual number of TCs generated over the WNP.

Collimore et al. (2003) discussed three mechanisms by which the QBO modulates the deep convection, including modulation of tropopause height, lower-stratospheric to upper-tropospheric zonal wind shear and upper-tropospheric relative vorticity. They suggested that the modulation of the cross-tropopause shear, which is measured by the monthly absolute value of the 50- to 200-hPa zonal wind shear, dominates the QBO-related convective behavior when the convection is concentrated away from the equator. Additionally, their results suggested that the modulation of the QBO may change between seasons and locations.

Therefore, it is interesting to address whether the cross-tropopause wind shear impacts convection over the WNP and the resultant influences on TC genesis in May. Moreover, it is important to investigate the combined impacts of ENSO and the QBO on TC genesis. This study is structured as follows. The data and methods are described in Sect. 2. The interannual correlation between the cross-tropopause wind shear and the number of TC genesis over the WNP in May is presented in Sect. 3. The different influences of the strong and weak cross-tropopause vertical wind shear on the changes in the tropical atmospheric circulation and convection over the WNP are investigated in Sect. 4. The combined impacts of ENSO and the QBO on TC genesis over the WNP in May and the corresponding energy conversions are analyzed in Sect. 5. Finally, the results are summarized and discussed in Sect. 6.

2 Data and methods

2.1 Data

(1) The TC data are obtained from the International Best Track Archive for Climate Stewardship (IBTrACS), including data during 1979–2015 (data version: v03r09) (Knapp et al. 2010), and the China Meteorological Administration–Shanghai Typhoon Institute, including data from 2016 (available at http://typhoon.nmc.cn/web.html). The interannual numbers of TCs over the WNP (0°–30°N, 110°–180°E) in May are counted, and the locations of TC genesis are identified when the storm intensity exceeds the tropical depression level. (2) The ERA-interim Reanalysis dataset provides the daily and monthly wind and temperature data at $2.5° \times 2.5°$ resolution during 1979–2016 (Simmons et al. 2007). (3) To verify the credibility of the stratospheric wind data from the ERA-Interim, zonal winds at 50 hPa during the period 1979–2016 from radiosonde observations in Singapore (1.22°N, 103.55°E) provided by the Free University of Berlin (http://www.geo.fu-berlin.de/met/ag/strat/produkte/qbo/qbo.dat) are employed. (4) The monthly mean outgoing longwave radiation (OLR) data during 1979–2013 with a $2.5° \times 2.5°$ resolution are derived from the National Oceanic and Atmospheric Administration (NOAA) archives (Liebmann 1996). The monthly mean OLR data for 2014–2016 are interpolated with Poisson's equation and reorganized based on the uninterpolated daily OLR data, which was also obtained from the NOAA archives (https://www.esrl.noaa.gov/psd/cgi-bin/db_search/DBSearch.pl?Dataset=NOAA+Uninterpolated+OLR&Variable=Outgoing+Longwave+Radiation). (5) The monthly SST data from 1979 to 2016 with a $1° \times 1°$ resolution are provided by the Met Office Hadley Centre's sea ice and sea surface temperature monthly mean datasets (Rayner et al. 2003).

2.2 Methods

In this study, the modulation of cross-tropopause wind shear is investigated by computing the monthly absolute value of the 50- to 200-hPa zonal wind shear following the work of Collimore et al. (2003). The El Niño events are identified when the Niño3 index is greater than 0.5 for 8 months, and the index is calculated as the normalized SST anomalies of the tropical eastern Pacific Ocean (5°S–5°N, 150°–90°W) (Feng et al. 2011). As the major cold ENSO episodes, La Niña events are identified when the Niño3 index is less than − 0.5 for 8 months. The interannual variations of Niño3 index are represented by the value obtained in January.

This study used the normalized stratospheric zonal wind at 50 hPa in May to represent the QBO. The QBO_W (QBO_E) is identified when the value is greater (less) than 0.8 (− 0.8). Correlation analysis is employed to investigate the interannual relationship between the number of TC genesis over the WNP in May and the cross-tropopause shear and related factors. To demonstrate the impact of the cross-tropopause shears on the changes in convection and the tropical atmospheric circulation over the WNP, composite analyses are performed based on the normalized time series of the cross-tropopause shear. Additionally, this method is employed to illustrate the combined impacts of ENSO and the QBO on TC genesis over the WNP in May. The correlation coefficient and the composite anomalies are assessed using Student's t-test. Moreover, the energy budget is analyzed with the barotropic eddy energy conversion equation following the work of Feng et al. (2014).

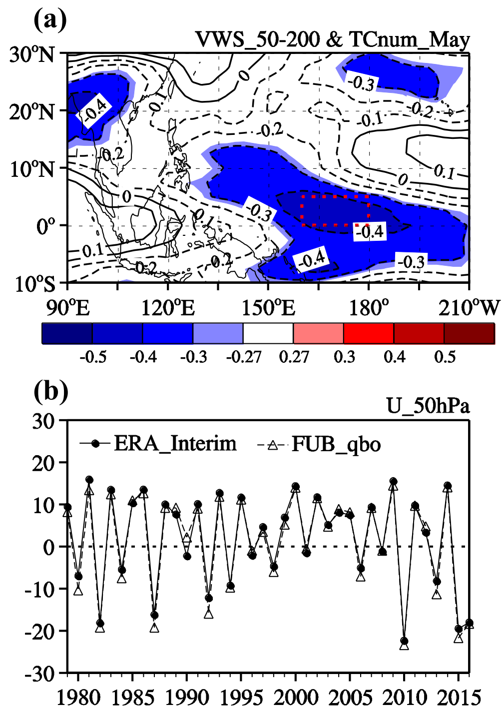

Fig. 1 **a** Correlation coefficients of the number of TC geneses over the WNP in May and the absolute value of the 50- to 200-hPa zonal wind shear. The red dashed black box denotes the key region (0°–5°N, 160°E–180°). **b** Time series of the zonal winds at 50 hPa derived from the ERA-Interim Reanalysis dataset (solid) and radiosonde observations from Singapore (dashed)

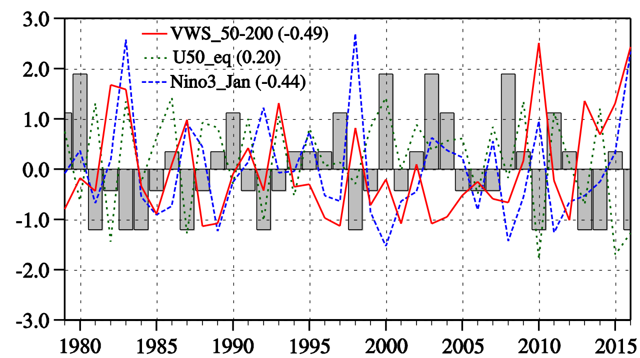

Fig. 2 Time series of the number of TC geneses over the WNP in May during 1979–2016 (bar graph). The red solid curve represents the cross-tropopause wind shear over the key region (0°–5°N, 160°E–180°), the dark-green dashed curve represents the zonal wind at 50 hPa at (0°, 165°E) in May and the blue dashed curve represents the January's Niño3 index during the same period

3 The interannual relationship between the cross-tropopause shear and the number of TCs generated over the WNP in May

The relationship between the cross-tropopause wind shear and the numbers of TCs generated over the WNP in May during 1979–2016 is studied in this section. The 50 hPa zonal wind analyzed in the cross-tropopause wind shear is extracted from the ERA-Interim dataset. To verify its credibility, we compared the data at 0°, 102.5°E with the radiosonde observations from Singapore (1.22°N, 103.55°E) (Fig. 1b). The stratospheric wind data from the ERA-interim Reanalysis data are quite consistent with the observations, with a correlation coefficient of greater 0.99. As shown in Fig. 1a, negative correlation coefficients are observed over the tropical Pacific. The significant negatively correlated band extends northwestward from the equator to the off-equator centered at approximately 0°–5°N, 160°–180°E. The correlation coefficients to the west of 120°E are insignificantly positive, indicating that the modulation of the cross-tropopause wind shear is not homogeneous over the tropics.

As noted above, the cross-tropopause shear over the tropical Central Pacific may play an important role in the modulation of TC genesis over the WNP in May. To investigate the interannual relationship between these systems, we compared the normalized time series of the number of TCs over the WNP in May and the cross-tropopause shear over the key areas (0°–5°N, 160°E–180°) which are obtained by dividing the interannual anomalies by each of their standard deviations (Fig. 2). This comparison indicates that the number of TCs in May is generally out of phase with the cross-tropopause shear with a significant correlation coefficient of

−0.49. Strong (weak) cross-tropopause shear over the tropical Central Pacific is related with a decreased (increased) TC genesis over the WNP in May. In addition, we have conducted a series of correlation analyses. The correlation coefficient between the number of TCs over the WNP in May and the stratospheric zonal wind at 50 hPa (QBO) in May is 0.20, whereas that between TC numbers and the January Niño3 index is −0.44. Hence, it is advisable to study the modulation of the stratospheric signals on TC genesis in May with the cross-tropopause shear instead of with the stratospheric winds or Niño3 index. We also performed correlation analyses between the cross-tropopause shear over the key area and the QBO in May and January Niño3 index, and the correlation coefficients are −0.44 and 0.52, respectively. That is, the weak (strong) cross-tropopause shear over the key area corresponds to the QBO_W (QBO_E) in most cases, which is consistent with the work of Gray et al. (1992). In addition, the weak (strong) cross-tropopause shear is correlated with the negative (positive) Niño3 index. The greater absolute value of the correlation coefficient between the cross-tropopause shear and the number of TCs over the WNP in May might indicate that the QBO signals can modulate the interannual relationship between the decaying El Niño (La Niña) events and TC genesis. Therefore, the cross-tropopause shear can be treated as a combined effect of ENSO and the QBO.

Notably, significant interannual variations in the normalized time series of the cross-tropopause shear have been observed. Therefore, we analyzed the main periods of this wind shear using wavelet analysis (figure not shown). The results showed that the main periods of this wind shear are focusing on the periods of 6–18 months. Therefore, the interannual correlation of the cross-tropopause shear and TC genesis over the WNP in May is relatively steady interdecadally, and the following analysis may derive more robust conclusions.

4 Influence of the cross-tropopause shear on the changes in tropical convections and atmospheric circulations

Composite analyses are performed to investigate the impact of cross-tropopause shear on the tropical convections and atmospheric circulations. The strong (weak) shear years are identified by requiring the normalized time series of the cross-tropopause shear in May to be no less (more) than 0.8 (−0.8). Nine strong shear years (1982, 1983, 1987, 1993, 1998, 2010, 2013, 2015 and 2016) and 9 weak shear years (1985, 1988, 1989, 1996, 1997, 2001, 2003, 2004 and 2012) were selected. Figure 3 presents composite figures of the OLR anomalies for the strong and weak shear years. In the strong shear years, the significantly weakened convections

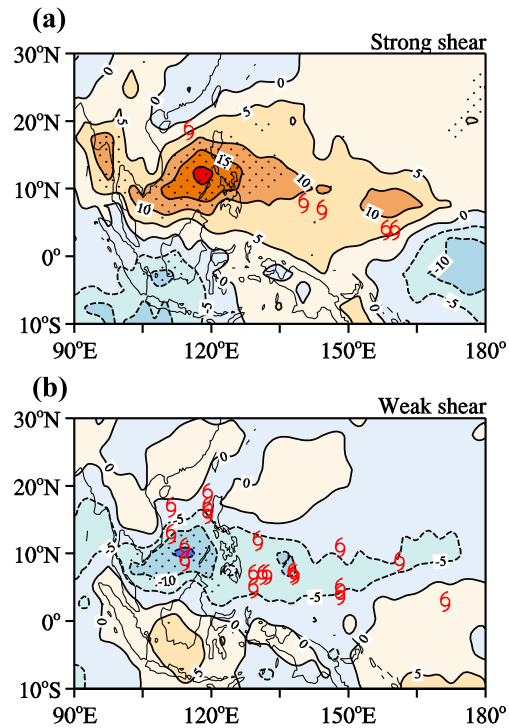

Fig. 3 Composite OLR (shading; units: Wm^{-2}) for **a** strong cross-tropopause shear and **b** weak cross-tropopause shear in May. The typhoon symbols indicate the locations of TC geneses. Stippling denotes anomalies significant at the 90% confidence level according to Student's t-test

are located around the SCS and the east of the Philippines (Fig. 3a). The positive OLR anomalies might result in late onset of the SCSSM (Huangfu et al. 2015). In such situations, the MT remained west, providing an unfavorable environment for TC genesis. In contrast, the convection over the tropics is significantly enhanced in the weak shear years (Fig. 3b). These OLR anomalies characterize a meridional tripole pattern with distributions reversed from those in the strong shear years. As mentioned above, most strong shear years are associated with the QBO_E, whereas the weak shear years correspond to the QBO_W. Therefore, the results indicated that the modulation of the cross-tropopause wind shear on convection over the WNP in May is more similar to the modulation of the QBO during the boreal summer (June–August), as described in the work by Collimore et al. (2003), than that during the spring (March–May).

As shown in Fig. 3a, b, the central anomalous OLR bands are displaced between 5° and 20°N in May. Hence, the zonal and vertical circulations averaged along the latitudinal band of 5°N–20°N are presented in Fig. 4. In this figure, the zonal and vertical wind fields are also composites based on the selected years as mentioned earlier. Concurrent with the strong cross-tropopause shear, significant anomalous descending motions are observed over the WNP, which

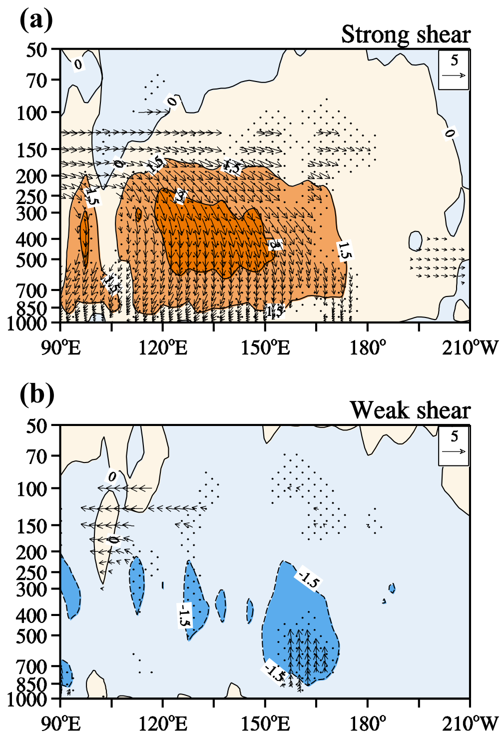

Fig. 4 Composite zonal and vertical velocities (vectors, units are m s^{-1} for u and 5×10^{-3} Pa s^{-1} for ω; shadings indicate the vertical velocities) averaged between 5°N and 20°N for **a** strong cross-tropopause shear and **b** weak cross-tropopause shear in May. The vectors shown and stippling denote the anomalies significant at the 90% confidence level according to Student's t-test

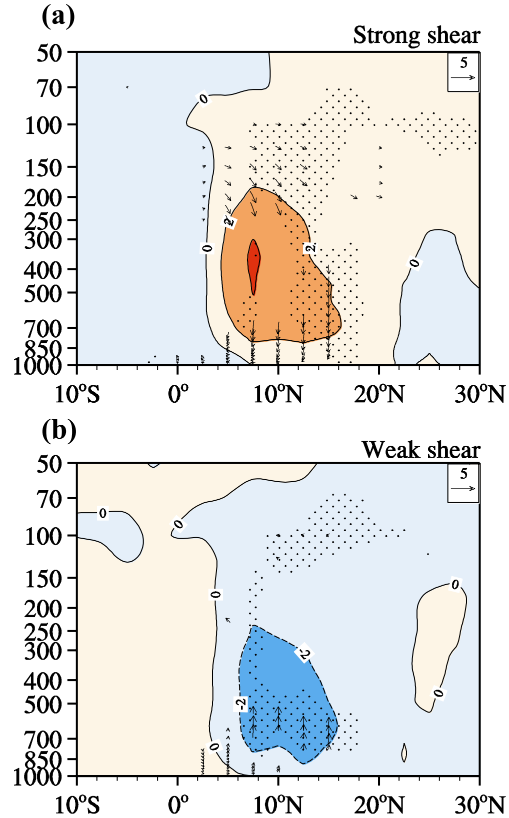

Fig. 5 Composite meridional and vertical velocities (vectors, units are m s^{-1} for v and 5×10^{-3} Pa s^{-1} for ω; shadings indicate the vertical velocities) averaged between 150°E and 170°E for **a** strong cross-tropopause shear and **b** weak cross-tropopause shear in May. The vectors shown and stippling denote the anomalies significant at the 90% confidence level according to Student's t-test

would weaken the updraft of the Walker circulation and the convection (Fig. 4a). In contrast, the weak shear leads to enhanced ascending motions, with relatively weak abnormal centers of vertical circulation over the WNP (Fig. 4b).

Moreover, considering the northwestward extension of the correlation distribution (Fig. 1a), the meridional and vertical circulations averaged along the longitudinal band of 150°–170°E are investigated in Fig. 5. The strong cross-tropopause shear over the eastern part of the WNP can lead to significant anomalous descending motions (Fig. 5a), centered at 5°–20°N, which is consistent with the results presented in Fig. 4a. In contrast, as shown in Fig. 5b, the weak shear leads to enhanced upward motions, favoring the convective activities. The meridional tripole patterns observed in Fig. 5a, b are consistent with the OLR anomalies presented in Fig. 3a, b.

We further compared four dynamic/thermodynamic factors to strengthen our argument. The differences between the strong and weak cross-tropopause shears (latter minus former) in the 850 hPa relative vorticities, the 200 hPa divergence, the 200–850 hPa vertical wind shear and the 700–500 hPa relative humidity are shown in Fig. 6. The low-level vorticity is always treated as one of the most important dynamic factors modulating TC genesis. As shown in Fig. 6a, the 850 hPa relative vorticity was largely strengthened over the SCS and the surrounding regions in the weak cross-tropopause shear years. As shown in Fig. 6b, significant upper-level divergence was observed over the tropics, which would reinforce the instability of atmosphere and tropical convection. Additionally, the vertical wind shear between 850 and 200 hPa over the WNP was investigated (Fig. 6c). Significantly weaker vertical wind shear was observed with a northwest–southeast orientation over the SCS and to the east of the Philippines. Note that the small vertical wind shear can help develop vertical convection, which is favorable for TC genesis. Moreover, we checked the 700–500 hPa relative humidity, which is an important thermodynamic factor for TC genesis (Fig. 6d). The results showed that the weak shear years can provide more abundant water vapor for TCs. These environmental factors are considered to be influenced by the cross-tropopause shears and responsible for the increase in TC genesis.

Affected by this cross-tropopause shear, we assessed the conditions of TC genesis in these two groups. The locations

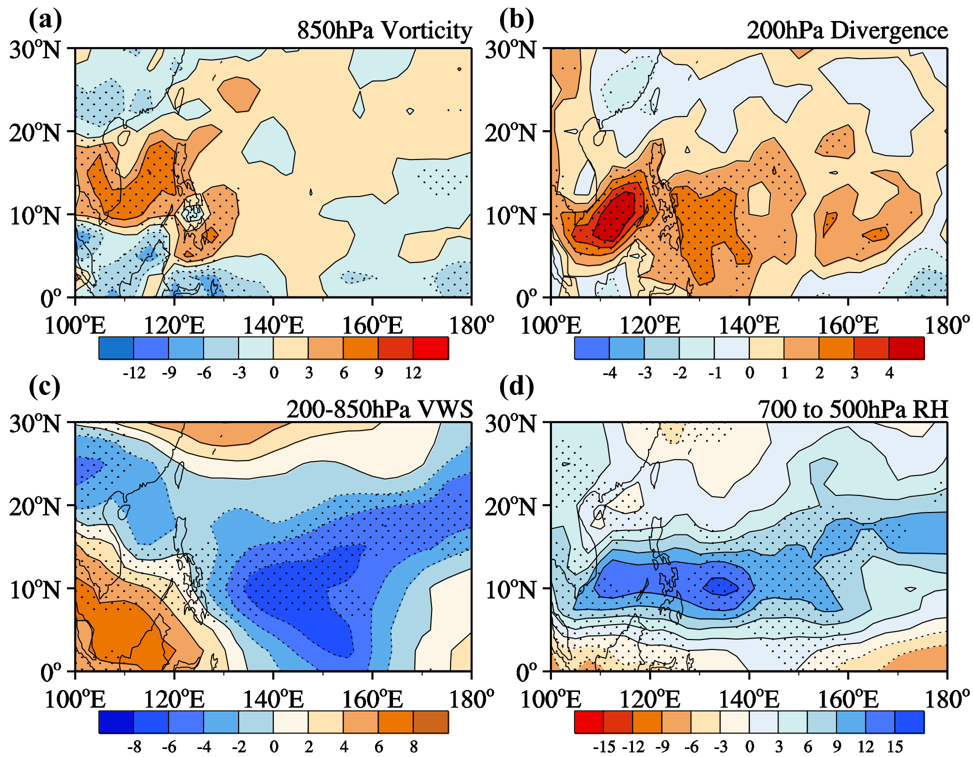

Fig. 6 The differences in the environmental factors in May between the strong and weak cross-tropopause shears (latter minus former): **a** the 850 hPa vorticity (units: 10^{-6} s^{-1}), **b** 200 hPa divergence (units: 10^{-6} s^{-1}), **c** 200–850 hPa vertical wind shear (units: m s^{-1}) and **d** 700–500 hPa relative humidity (units: %)

of TCs are following the MT zone. According to statistics, sixty TCs were generated over the WNP in May during 1979–2016, with approximately 1.6 TCs per year on average (figure not shown). The 5 TCs generated in the nine strong shear years are less than average, whereas the 19 TCs generated in the 9 weak shear years are above average.

5 Combined impacts of the QBO and ENSO on TC genesis over the WNP in May and the corresponding energy conversions

The impact of the QBO on TC genesis is indirect. QBO may play a more substantial role when it is coupled with ENSO events. According to Du et al. (2011), poor TC genesis was observed in strong El Niño decaying summers. The present study expanded the investigation to moderate El Niño events and sought to further verify the influence of El Niño events with more cases. The relationship between the Niño3 index and TC genesis number in May was investigated. The result indicates that their correlation coefficient is -0.40. This significant robust correlation means that even moderate ENSO events can influence TC genesis in May, which is our emphasis in the present study. Additionally, we wanted to examine the conditions in the decaying La Niña years. Based on the time series of the Niño3 index, nine El Niño decaying years (1983, 1987, 1988, 1992, 1998, 2003, 2007, 2010 and 2016) and ten La Niña decaying years (1985, 1986, 1989, 1996, 1999, 2000, 2001, 2008, 2011 and 2012) are identified. Figure 7 presents the composite figures of OLR and the 850-hPa streamline, and the TCs in May and the 5880 gpm lines at 500 hPa (representing the western Pacific subtropical high (WPSH)) were superimposed. Regarding the nine El Niño decaying years, only seven TCs were generated, which is significantly less than the average number (1.6 TCs per year) (Fig. 7a). The tropical convections were significantly suppressed in the low latitudes, and the anomalous wind fields were anti-cyclonic. The 5880 gpm line was shown over the SCS and to the east of the Philippines, meaning that the WPSHs were stronger in these years than in normal years. The strong WPSH led to late onset of the SCSSM and weak eastward extensions of the MT, which induced less favorable environments for TC genesis in May. This result is consistent with the work of Du et al. (2011). As shown in Fig. 7b, the composite analysis is based on ten La Niña decaying years. Twenty-two TCs were generated over the WNP, which is a greater number than the average. Significant anomalous southwesterly winds are observed in the low latitudes, meaning the MT can extend farther east. The 5880 gpm lines at 500 hPa shrank to a small area around approximately 24°N, 160°E, meaning that the WPSHs were much weaker in the La Niña decaying years than in normal years.

To investigate the combined impacts of ENSO and the QBO on TC genesis over the WNP in May, four El Niño decaying years coupled with QBO_E (1987, 1992, 2010 and

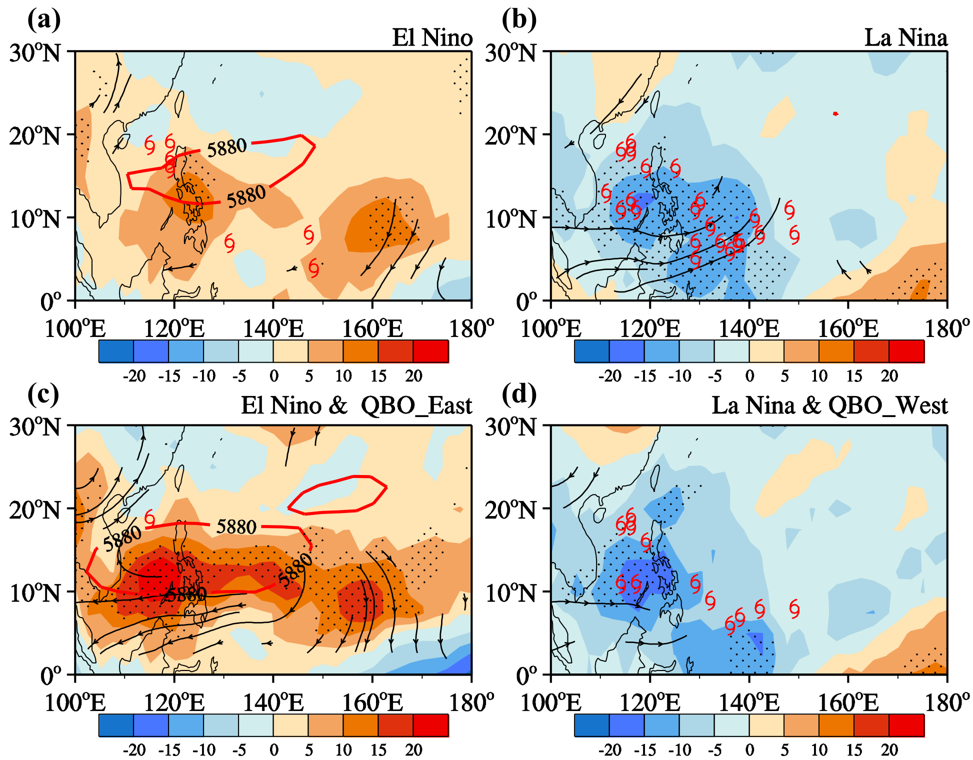

Fig. 7 Composite 850 hPa horizontal wind field (streamline) and OLR (shading; units: Wm^{-2}) in May for **a** decaying El Niño events, **b** decaying La Niña events, **c** decaying El Niño events coupled with the QBO_E, and **d** decaying La Niña events coupled with the QBO_W. The typhoon symbols indicate the locations of TC geneses and the solid red lines indicate the 500 hPa 5880 gpm delineations. The streamline and stippling denote anomalies significant at the 90% confidence level according to Student's t-test

2016) and six La Niña decaying years coupled with QBO_W (1985, 1986, 1989, 1999, 2000 and 2011) were further identified. The number of TC genesis exhibits notable contrasts between these two groups. Only 1 nameless TC was generated during the four El Niño and QBO_E years (Fig. 7c). Greater positive OLR anomalies are observed, with the 850 hPa anomalous anti-cyclones controlling the southwest quadrant of the WNP. The coverage of the 5880 gpm line was significantly enlarged compared with the situation in Fig. 7a. The QBO_E might modulate the influence of the decaying El Niño events on TC genesis in May by weakening the tropical convection. The combined impacts of decaying El Niño events and the QBO_E led to weaker TC genesis in May. In this group, 1987, 2010 and 2016 are also listed in the strong shear years, indicating that the strong shears are largely related with the decaying El Niño events and the QBO_E. In contrast, when La Niña decaying years are coupled with QBO_W phase, the distribution of the positive OLR anomalies shifted more westward, with greater amplitude but smaller coverage (Fig. 7d). The anomalous wind fields are significantly less during El Niño years than during La Niña years, as shown in Fig. 7b. The mean strengths of the WPSH on the 500 hPa geopotential level is weaker than those with 5880 gpm. Twelve TCs were generated in this group, and the annual mean is basically equal to that in La Niña years. Compared with the weak cross-tropopause shear years, most of the weak shear years are related to La Niña events (1985, 1996, 2001 and 2012). The modulation of the QBO_W on La Niña events is limited, with only 1989 included. This result may indicate that the modulation effects of the QBO on different ENSO events are asymmetric. The combined impacts of the decaying El Niño events and the QBO_E are more influential to the cross-tropopause shear and thus suppresses TC genesis over the WNP in May.

By affecting tropical convections and the atmospheric circulations, the combined impacts of ENSO and the QBO may change the energy conversion in the formation of TCs. The energy analysis would help explain the dynamic processes of TC genesis in May over the WNP. Given that the atmosphere is barotropically unstable in the tropics, the TC genesis processes are concurrent with the barotropic kinetic energy conversion (Feng et al. 2014). The barotropic eddy kinetic conversion equation deduced by Maloney and Hartmann (2001) is employed to investigate these processes.

$$\frac{\partial}{\partial t}K'_{baro} = -\overline{u'v'}\frac{\partial}{\partial y}\overline{u} - \overline{u'v'}\frac{\partial}{\partial x}\overline{v} - \overline{u'^2}\frac{\partial}{\partial x}\overline{u} - \overline{v'^2}\frac{\partial}{\partial y}\overline{v} \qquad (1)$$

In Eq. (1), u and v are the horizontal zonal and meridional winds, respectively. K_{baro} denotes barotropic eddy kinetic energy, which equals $(u^2+v^2)/2$. $\overline{A}$ denotes the mean state variables and A' denotes the anomalous variables by subtracting the mean state. K'_{baro} denotes the horizontal barotropic eddy kinetic energy (EKE). $\frac{\partial}{\partial t}K'_{baro}$ indicates the "tendency of the barotropic EKE", which represents the rate of change of the horizontal barotropic EKE conversion. Climatologically, the MTs are the most active region where the energy from the mean flow was converted into barotropic EKE, with the positive conversion extending southeastward from the SCS region (figure not shown). In El Niño decaying years, the barotropic EKE conversion is relatively weaker over most parts of the tropics (Fig. 8a). As mentioned above, the El Niño-related anti-cyclones in May can lead to the late onset of the SCSSM and the late intrusion of the MT into the WNP. Hence, MT-related barotropic energy conversions were weak in these years. Concurrent with the QBO_E, an even weaker barotropic EKE conversion is observed (Fig. 8c). This result indicates that the QBO_E may enhance the El Niño-related anti-cyclone and restrict the eastward extension of the MT, leading to suppressed energy conversion to support TC genesis. Therefore, only one nameless TC was generated in the four decaying El Niño and QBO_E years. In contrast, the barotropic energy conversions were stronger in the La Niña decaying years (Fig. 8b). Even stronger barotropic EKE conversions are observed in the six decaying La Niña and QBO_W years at low latitudes (Fig. 8d).

The right-hand side of the barotropic eddy kinetic conversion equation includes four terms: meridional shear of the mean zonal winds, zonal shear of the mean meridional winds, zonal wind convergence, and meridional wind convergence. The terms are typically explored to examine what type of circulation contributes more to the barotropic EKE conversions. $-\overline{u'v'}\frac{\partial}{\partial y}\overline{u}$ denotes the meridional shear of the mean zonal winds. The climatological contribution of this term is confined to the low latitudes because the contribution of this term is mostly attributed to the trough line of the MT. In the years following El Niño events, the easternmost location of the MT remains to the west, and the anomalous barotropic EKE conversion is negative over most parts of the tropics (Fig. 9a). In the cases shown in Fig. 7b, c, the MT was confined in the west. The conversion shown in Fig. 9c exhibits a similar distribution to that in Fig. 9a. This finding is consistent with the environment shown in Fig. 7c, where the combined impacts of the decaying El Niño events and the QBO_E enhanced the WPSH and suppressed convection over the tropical WNP. In contrast, the intrusion of the MT in the La Niña decaying years promotes increased EKE conversion eastward (Fig. 9b). When La Niña decaying events are coupled with the QBO_W, greater EKE conversion can be observed in the tropics (Fig. 9d). Note that the amplitudes of the first term presented in Fig. 8 are approximately half of those in Fig. 8.

The third term $-\overline{u'^2}\frac{\partial}{\partial x}\overline{u}$ denotes the zonal wind convergence, which is typically located eastward ahead of the MT with the convergent area between the southwesterly and easterly trade winds. The EKE conversion exhibits wider coverage and greater amplitudes than those in the first term, contributing more to the EKE tendencies (figure not shown). Given that the MT remained in the west in the El Niño decaying years and the El Niño and QBO_E years, Fig. 10a, c resemble the distributions of Fig. 9a, c, with relatively

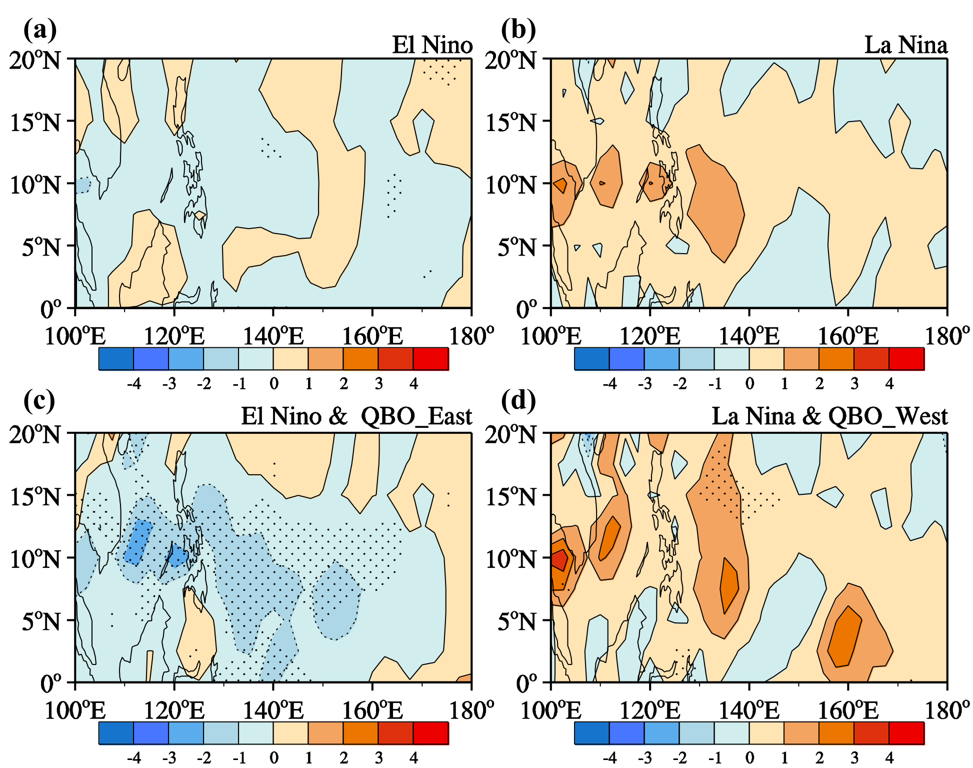

Fig. 8 Composite 850 hPa temporal rates of change of the EKE (units: 10^{-5} m^2 s^{-3}) in May for **a** decaying El Niño events, **b** decaying La Niña events, **c** decaying El Niño events coupled with the QBO_E, and **d** decaying La Niña events coupled with the QBO_W. Stippling denotes the anomalies significant at the 90% confidence level according to Student's t-test

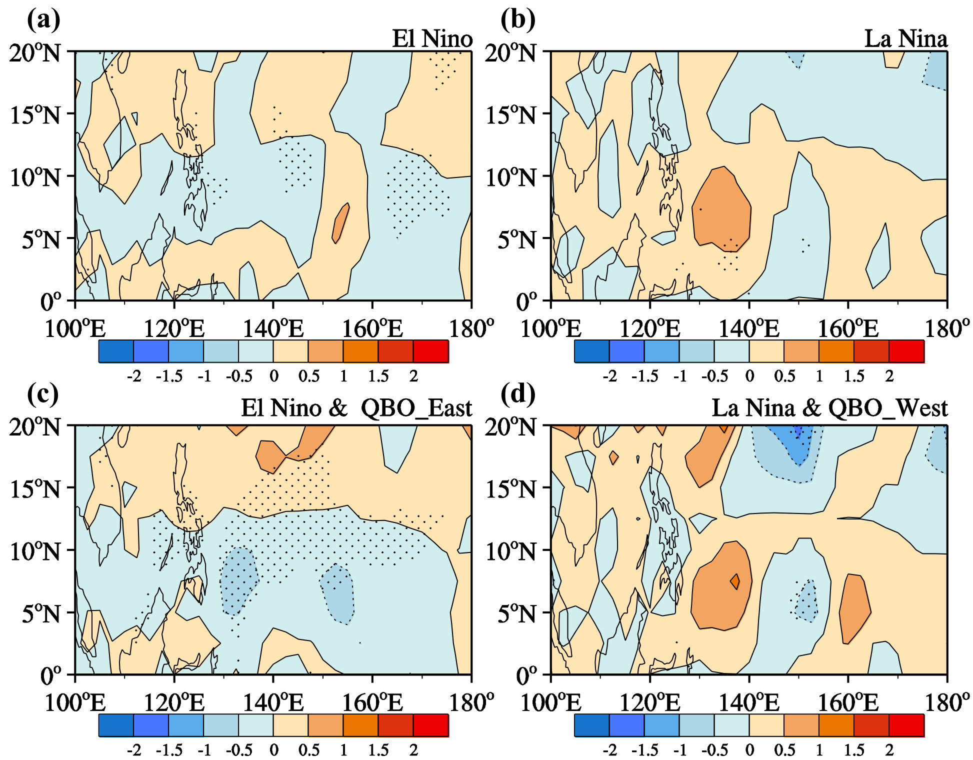

Fig. 9 Composite 850 hPa horizontal distributions of the meridional shears of the zonal wind term (units: 10^{-5} m^2 s^{-3}) in May for **a** decaying El Niño events, **b** decaying La Niña events, **c** decaying El Niño events coupled with the QBO_E, and **d** decaying La Niña events coupled with the QBO_W. Stippling denotes anomalies significant at the 90% confidence level according to Student's t-test

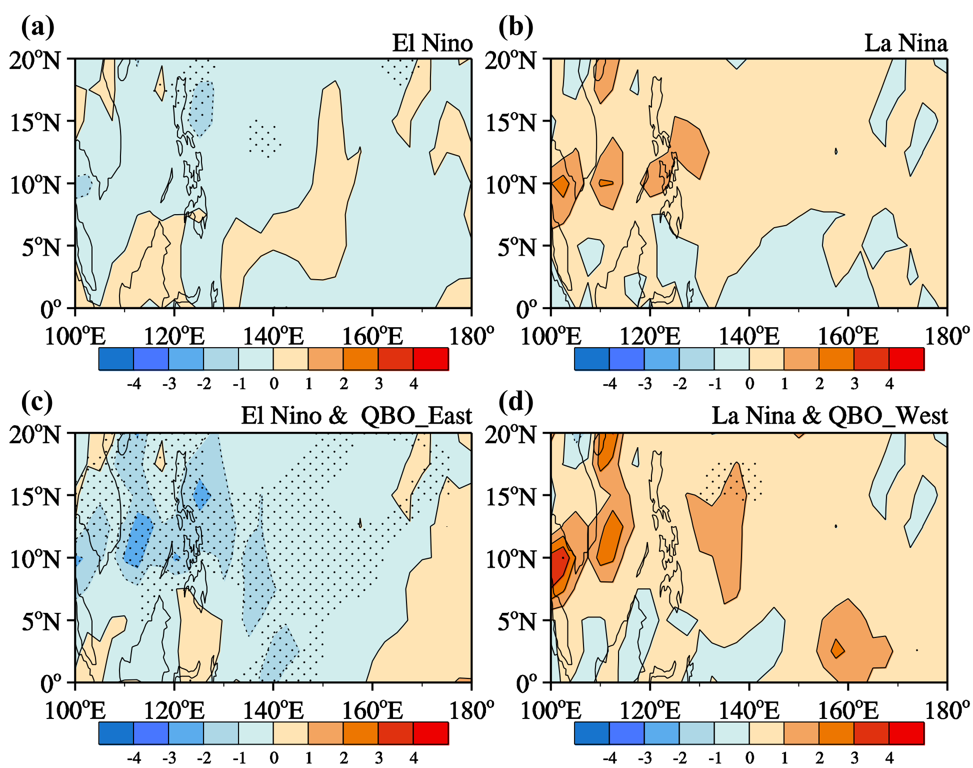

Fig. 10 Composite 850 hPa horizontal distributions of the zonal wind convergence term (units: 10^{-5} m^2 s^{-3}) in May for **a** decaying El Niño events, **b** decaying La Niña events, **c** decaying El Niño events coupled with the QBO_E, and **d** decaying La Niña events coupled with the QBO_W. Stippling in **c** denotes anomalies significant at the 90% confidence level according to Student's t-test

small contributions to the EKE tendencies. Contrasted with the above cases, the contribution of the zonal wind convergence is considerable in La Niña decaying years (Fig. 10b). With the eastward extension of the MT, greater contributions from the zonal wind convergences are observed in the low latitudes. The combined effect of La Niña and QBO_W enlarged this EKE conversion slightly (Fig. 10d). Given that only a portion of the MT can enter the WNP in May, the contribution of the meridional shear of the mean zonal winds is less important than that of the zonal wind convergence. This result is different from previous studies that demonstrated that the contributions of the first terms carry greater importance in the peak TC season (Feng et al. 2014; Wu et al. 2015). These results may further indicate that TC genesis over the WNP in May exhibits distinct characteristics. In addition, the second term (the zonal shear of the mean meridional winds) and the fourth term (the meridional convergence of the mean meridional winds) are negligibly small in the analysis (figures not shown).

6 Summary and discussion

This study investigates the role of the cross-tropopause wind shear in the modulation of TC genesis over the WNP in May. Correlation analysis results indicate that TC genesis in May is negatively correlated with the cross-tropopause wind shear over the southeastern WNP and the Central Pacific during 1979–2016. The key regions stretch northwestward to approximately 130°E. Moreover, wavelet analysis of this cross-tropopause shear indicates that the variations in the cross-tropopause shear are mainly interannual. Therefore, the correlations between the cross-tropopause shear and TC genesis over the WNP in May are relatively steady.

Composite analysis reveals that the modulation by the strong cross-tropopause wind shear on the tropical convection in May is similar to the modulation of the QBO on the boreal summer (June–August), as described in the work of Collimore et al. (2003), instead of that during the spring (March–May). Concurrent with the strong shear, significant weak convection anomalies are observed over the tropical WNP, especially over the SCS and to the east of the Philippines. In contrast, stronger convection corresponds to weak shear. Further analysis revealed that the strong cross-tropopause shear may weaken the convection over the warm pool and lead to suppressed vertical motions centered at 5°N–20°N. In addition, the weak shear leads to enhanced convection, with enhanced ascending motions over the WNP, which favor tropical convection. The TCs generated in the strong and weak shear years exhibit notable contrasts. Only 5 TCs were generated in the nine strong shear years, whereas 19 TCs were generated during the 9 weak shear years.

According to our analysis, the cross-tropopause shear is not independent from the QBO and ENSO events. The QBO signals might modulate the interannual relationship between decaying ENSO events and TC genesis. The cross-tropopause shear can be treated as a combined effect of ENSO and the QBO. As suggested by Du et al. (2011), fewer TCs will be generated in the years following strong El Niño events. This study expanded the investigation to moderate El Niño events and examined the modulation by the QBO_E. The results revealed that TC genesis in May following El Niño events is significantly weaker than normal. With the WPSH remaining strong and stretched to the west in May, fewer TCs were generated. This suppression is intensified when coupled with the QBO_E. Stronger WPSH was observed, with the 850 hPa anomalous anti-cyclone controlling the tropical WNP. The convection over the tropical WNP was even weaker. Only one nameless TC was generated in these years. In contrast, following La Niña events, different distributions of anomalous convections and tropical circulations are observed. The convection was enhanced, and the WPSH was significantly weakened. A greater number of TCs was generated over the WNP. This situation was enhanced when the decaying La Niña events were coupled with the QBO_W.

In addition, concurrent with the different atmospheric responses, barotropic kinetic energy conversions are analyzed to reveal the internal dynamics of the modulations from the combined effect of ENSO and the QBO. In the years following the El Niño events, the El Niño-related anti-cyclones in May led to late eastward extensions of the MT, and the MT-related barotropic energy conversions were accordingly weak. Given that MTs rarely intrude into the WNP in May, the combined impacts of the decaying El Niño events and the QBO_E on the EKE conversions are significant, with considerably weak amplitudes in both the contributions of the meridional shear of the mean zonal winds and the zonal wind convergence. In contrast, the cases following La Niña events exhibited significantly enhanced EKE conversions in the lower tropics, favoring increased numbers of TC genesis over the WNP in May. When coupled with the QBO_W, the EKE conversion was enhanced slightly. Compared with the cross-tropopause shear years, the combined impacts of the decaying El Niño events and the QBO_E are more influential to the strong cross-tropopause shear and thus the suppression of TC genesis, whereas the modulation of the QBO_W on decaying La Niña events is limited.

Tropical cyclone genesis over the WNP in May is sensitive to the eastward extension of the MT. Hence, in addition to ENSO and the QBO, other important climate events may induce changes in TC genesis in May by affecting the MT and MT-related energy conversions. Previous studies have shown that El Niño developing years can also influence TC activity (Lander 1994; Chen et al. 1998). The mean TC genesis location tended to shift more southeastward and would lead to a slight increase in the numbers of TCs in El Niño developing summers. Clark and Chu (2002) revealed that the changes in TC activity are related to the eastward extension in El Niño developing years, which is quite different from the situation in El Niño decaying years. In addition, studies have focused on the influences of the central Pacific (CP) El

Niño and the eastern Pacific (EP) El Niño events. Wu et al. (2018) suggested that the influence of the extreme EP El Niño is similar to that of the CP El Niño, leading to a notable southeastward shift in TC genesis locations. These changes are clearly different from the effects of moderate EP El Niño and weak EP El Niño events. Therefore, further elaborations regarding the modulation of the QBO on different ENSO events are also needed in future studies.

Acknowledgements This work was supported by the National Key Research and Development Program of China (2016YFA0600603), and the National Natural Science Foundation of China (Grant nos. 41705071, 41661144016, 41461164005, 41375065, 41230527).

References

Baldwin MP et al (2001) The quasi-biennial oscillation. Rev Geophys 39:179–229

Camargo SJ, Sobel AH (2010) Revisiting the influence of the quasi-biennial oscillation on tropical cyclone activity. J Clim 23:5810–5825

Caron L-P, Boudreault M, Camargo SJ (2015) On the variability and predictability of eastern Pacific tropical cyclone activity. J Clim 28:9678–9696

Chan JCL (1995) Tropical cyclone activity in the western north Pacific in relation to the stratospheric quasi-biennial oscillation. Mon Weather Rev 123:2567–2571

Chen T-C, Weng SP, Yamazaki N, Kiehne S (1998) Interannual variation in the tropical cyclone formation over the Western North Pacific. Mon Weather Rev 126:1080–1090

Chen T-C, Tsay J-D, Matsumoto J, Alpert J (2017) Impact of the summer monsoon westerlies on the South China Sea tropical cyclone genesis in may. Weather Forecast 32:925–947

Clark JD, Chu PS (2002) Interannual variation of tropical cyclone activity over the central north pacific. J Meteorol Soc Jpn 80:403–418

Collimore CC, Martin DW, Hitchman MH, Huesmann A, Waliser DE (2003) On the relationship between the QBO and tropical deep convection. J Clim 16:2552–2568

Du Y, Yang L, Xie S-P (2011) Tropical Indian ocean influence on northwest Pacific tropical cyclones in summer following strong El Niño. J Clim 24:315–322

Fadnavis S, Ernest Raj P, Buchunde P, Goswami BN (2014) In search of influence of stratospheric Quasi-Biennial Oscillation on tropical cyclones tracks over the Bay of Bengal region. Int J Climatol 34:567–580

Feng J, Chen W, Tam CY, Zhou W (2011) Different impacts of El Ni o and El Ni o Modoki on China rainfall in the decaying phases. Int J Climatol 31:2091–2101

Feng T, Chen G-H, Huang R-H, Shen X-Y (2014) Large-scale circulation patterns favourable to tropical cyclogenesis over the western North Pacific and associated barotropic energy conversions. Int J Climatol 34:216–227

Goebbert KH, Leslie LM (2010) Interannual variability of northwest Australian tropical cyclones. J Clim 23:4538–4555

Gray WM (1984) Atlantic seasonal hurricane frequency. Part I: El Niño and 30 mb quasi-biennial oscillation influences. Mon Weather Rev 112:1649–1668

Gray WM, Sheaffer JD, Knaff JA (1992) Influence of the stratospheric QBO on ENSO variability. J Meteorol Soc Jpn 70:975–995

He H, Yang J, Gong D, Mao R, Wang Y, Gao M (2015) Decadal changes in tropical cyclone activity over the western North Pacific in the late 1990s. Clim Dyn 45:3317–3329

Ho C-H, Kim H-S, Jeong J-H, Son S-W (2009) Influence of stratospheric quasi-biennial oscillation on tropical cyclone tracks in the western North Pacific. Geophys Res Lett 36:L06702. https://doi.org/10.1029/2009gl037163

Huangfu J, Huang R, Chen W (2015) Influence of tropical western Pacific warm pool thermal state on the interdecadal change of the onset of the South China Sea summer monsoon in the late-1990s. Atmos Oceanic Sci Lett 8:95–99

Huangfu J, Huang R, Chen W (2017a) Interdecadal increase of tropical cyclone genesis frequency over the western north Pacific in May. Int J Climatol 37:1127–1130

Huangfu J, Huang R, Chen W (2017b) Relationship between the South China Sea summer monsoon onset and tropical cyclone genesis over the western North Pacific. Int J Climatol 37:5206–5210

Huangfu J, Chen W, Ma T, Huang R (2017c) Influences of sea surface temperature in the tropical Pacific and Indian Oceans on tropical cyclone genesis over the western North Pacific in May. Clim Dyn. https://doi.org/10.1007/s00382-017-3989-y

Jury MR, Pathack B, Parker B (1999) Climatic determinants and statistical prediction of tropical cyclone days in the southwest Indian ocean. J Clim 12:1738–1746

Knapp KR, Kruk MC, Levinson DH, Diamond HJ, Neumann CJ (2010) The international best track archive for climate stewardship (IBTrACS) unifying tropical cyclone data. Bull Am Meteorol Soc 91:363–376

Lander MA (1994) An exploratory analysis of the relationship between tropical storm formation in the western north Pacific and ENSO. Mon Weather Rev 122:636–651

Liebmann BCAS (1996) Description of a complete (interpolated) outgoing longwave radiation dataset. Bull Am Meteorol Soc 77:1275–1277

Liu KS, Chan JC (2013) Inactive period of western North Pacific tropical cyclone activity in 1998–2011. J Clim 26:2614–2630

Maloney ED, Hartmann DL (2001) The Madden–Julian oscillation, barotropic dynamics, and north Pacific tropical cyclone formation. Part I: observations. J Atmos Sci 58:2545–2558

Rayner N et al. (2003) Global analyses of sea surface temperature, sea ice, and night marine air temperature since the late nineteenth century. J Geophys Res Atmos (1984–2012) 108:D14,4407. https://doi.org/10.1029/2002JD002670

Shapiro LJ (1989) The relationship of the quasi-biennial oscillation to Atlantic tropical storm activity. Mon Weather Rev 117:1545–1552

Simmons A, Uppala S, Dee D, Kobayashi S (2007) ERA-Interim: new ECMWF reanalysis products from 1989 onwards. ECMWF newsletter 110:25–35

Wu L, Wen Z, Wu R (2015) Influence of the monsoon trough on westward-propagating tropical waves over the western north Pacific. Part II: energetics and numerical experiments. J Clim 28:9332–9349

Wu L, Zhang H, Chen J-M, Feng T (2018) Impact of two types of El Nino on tropical cyclones over the western north Pacific: sensitivity to location and intensity of pacific warming. J Clim 31:1725–1742

Xie S-P, Hu K, Hafner J, Tokinaga H, Du Y, Huang G, Sampe T (2009) Indian ocean capacitor effect on Indo–Western Pacific climate during the summer following El Niño. J Clim 22:730–747